Performance Studies of Alumina TiC-based Ceramic Tool Inserts when Turning Tool Steels

V.C.Venkatesh, Z.A.Ahmad and M.Konneh

Faculty of Mechanical Engineering, Universiti Teknologi Malaysia,
81310 UTM, Skudai, Johor Bharu, Malaysia

Abstract

Investigation in this paper is devoted to evaluating the cutting performance of two alumina TiC-based ceramic cutting tools having negative side cutting edge angles (SCEA)s of -5^0 (CNG) and -1^0 (TNG) by finish turning two tool steels. Experimental studies were carried out at various cutting speeds, feeds and depths of cut in dry conditions. The cutting performance of the alumina-based ceramic tools was judged by the cutting force produced during the process of machining and by the surface roughness of the workpieces. The influence of the cutting parameters (that is, the cutting speed, feed and depth of cut) on the cutting performance is discussed. The higher negative SCEA of -5^0 generally works better for the tool steels than the -1^0. Turning with ceramics compares favourably with alternative machining processes normally used in the fabrication of die and moulds.

Keywords: Ceramic cutting tools, alumina, surface roughness, cutting force, tool performance, turning, tool steels

1 Introduction

To achieve the desired production and economic advantages in aerospace, automotive and steel industries, more refractory cutting tools like ceramics are required. The refractory nature of Al_2O_3 ceramic tools coupled with their high wear resistance, high compression strength, has necessitated their use at much higher speeds than possible with cemented carbides [1]. Although ceramic tool materials have certain specialized properties, which necessitate their use for high speed machining and hard-part turning, they have certain drawbacks. The mechanical and thermal properties, low toughness being the major deficiency of the tools subject them to an unpredictable tool performance, which is undesirable in today's manufacturing undertakings. Strength, thermal shock resistance, and particularly impact resistance are usually the limiting factors in the performance of ceramic tools as reported by Whitney [1]. His work further reported that low bulk toughness and thermal conductivity of the tools result in low resistance to mechanical and thermal shocks respectively. Also the susceptibility to mechanical shock and vibration is a result of low impact i.e. low tensile strength in the materials. The low or poor resistance to the mechanical and thermal shocks results in an unpredictable performance of the tools. Such unpredictable tool behavior can, at times, cause poor machinability [2, 3]. These characteristics have limited the use of ceramic tools in a number of varied machining applications such as turning, milling, etc.

Al_2O_3-based tools especially have low heat conductivity values [4], low toughness resulting in brittle fracture (chipping) which, may cause unpredictable surface finish, and the low mechanical resistance to bending (low tensile strength) may prevent them from withstanding cutting forces. Kalpakjian [4] reported that Tool and Die steels, as a class of hard materials, are very difficult to machine and usually require annealing prior to machining. One of the alloying elements in steel, silicon combines with oxygen in the air to form silicates. These compounds are hard and abrasive, thus resulting in relatively poor machinability. Other alloying elements such as Ni, Cr, Mo, and V, which improve the properties of steels, generally reduce machinability.

Shaw [5] have considered finish turning operations as operations typically performed under a depth of cut of 1.5 mm and feed less than 0.15 mm/rev. Jawahir et al. [6] undertook an experimental study on finish turning of steels with cermet chip turning inserts. Three major machinability parameters: chip breakability, surface roughness and specific cutting force, were investigated. The interrelationship among these parameters was established with a view to developing methodology for optimum solutions in finish turning operations. The basic analysis presented a new method for determining the chip breakability level and the achievable surface roughness, R_a for a given chip groove, work material and a set of cutting conditions (feed, depth of cut, cutting speed). In their work, tool wear was considered insignificant, although the three machinability parameters investigated would have been affected by progressive tool-wear which, in general, also reduces machining accuracy. The reason for this being that the actual machining time for producing the required tests was only small and that new cutting edges were used for each depth of cut considered, in effect allowing a total of no more than 30-40 seconds of the machining using each cutting edge.

Venkatesh et al [7] analyzed the cutting performance of three 80^0 diamond shaped inserts with SCEAs of -5^0, 0^0, and $+15^0$ by machining low carbon steel (1018) at speeds of 450, 560, and 710 sfm, depth of cut 0.1 mm and feed 0.01 ipm. Cutting forces were measured, and friction and shear plane angles determined. Chips and chip roots were analyzed using digital image techniques. Surface roughness and roundness, brightness measurements were made. The results indicated that the tool with -5^0 SCEA performed better than the other two.

Organizations confronted with the problem of developing cutting tool materials manifest keen interests to evaluating the tool materials, or tests are also required to enable cutting tool materials to be evaluated. The development of new or improved cutting tools requires the evaluation of these tools' performance to classify their range of application and to get hints for further developments. The performance of a cutting tool can be assessed by factors such as cutting force, specific cutting force, cutting temperature, surface finish, and tool wear. Investigation in this paper is devoted to evaluating the cutting performance of alumina TiC-based ceramic cutting tools having negative side cutting edge angles (SCEA) of -5^0 (CNG) and -1^0 (TNG) by finish turning two tool steels. Evaluation of the cutting performance of the alumina-based ceramic tools was judged by the cutting force produced during the process of machining and by the surface roughness of the workpieces. The effect of tool wear was assumed insignificant in this work. The actual turning time for producing the required tests was very small, not permitting the continuous turning process to exceed more than 10 seconds in each cutting experiment, in effect a total of less than 40 seconds of the machining using each cutting edge [6]. Milling, grinding and EDM tests were carried out so as to compare the surface roughness generated during the turning operations with alternative metal cutting processes, to demonstrate that ceramics could be used in die and mould making.

2 Experimental Methods

2.1 Experimental Set-up

a) Lathe. Model: Harrison M500 with spindle RPM 1600 (max.), feed range of 0.04-0.71 mm/rev; and motor HP: 12.6 i.e. 9.3 KW.
b). Three-component tool dynamometer. Model: KISTLER Type: 9265B; calibrated range: Fx (=Ff) = 0-15000 N;
Fy (=Fp) = 0-15000 N; Fz (=Fc) = 0-30,000 N
c) Multichannel charge amplifier: KISTLER Type: 5019A.
d) The data acquisition module. This consists of IBM Personal computer as controller, IEEE cable for PC-charge amplifier connection, ASYST Runtime License, connecting cable for Multichannel equipment data-acquisition card, 1 parallel for printer (LPT 1), EPSON compatible Printer.
e) Surface roughness-measuring equipment. MITUTOYO SURFTEST 301.
f) Optical microscope
g) Torque Wrench

2.2 Work Materials

The workpiece materials investigated were High carbon high chromium steel (XW-42); AISI = D2, JIS = SKD = 11; Chemical composition: C = 1.55%, Si = 0.30%, Mn = 0.30%, Cr = 12%, Mo = 0.80%, V = 0.80%, 210 HB. Powdered high speed steel (ASP-23); AISI = M3:2, JIS = SKH = 54; Chemical composition : C = 1.27%, Si = 0.30%, Mn = 0.30%, Cr = 4.2%, Mo = 5.00%, V = 3.10%, W = 6.4%, 260 HB. The XW-42 was 50.8 mm in diameter and 337 mm in length and the ASP-23, 25.4 mm and 337 mm in diameter and length respectively.

2.3 Tool Inserts

Alunima TiC-based (Al_2O_3 = 70%, TiC = 30%) -5^0 SCEA (CNG) and -1^0 SCEA (TNG) tool inserts manufactured by SANDVIK cutting tool manufacturers were used in the experimental work. Toolholders were CCLNR 2525M 12 IC and CTGNR 2525M 16 ID. Tool angles were -1^0 SCEA (TNG): -6, -6, 6, 6, 29, -1, 0.8 and -5^0 SCEA (CNG): -5, -5, 5, 5, 5, -5, 0.8.

2.4 The Cutting Conditions

The cutting conditions for the first set of experiments by the traditional method are as follows:

Cutting speed: 77, 97, 123, 154, 192, 250 m/min for the work material High carbon high chromium steel (XW-42) and 50, 64, 80, 100, 126 m/min for material Powdered high speed steel (ASP-23). Feed: 0.05, 0.08, 0.125, 0.18, 0.23 mm/rev for material XW-42; 0.04, 0.05, 0.08, 0.125, 0.18, 0.23 mm/rev for the material ASP-23. Depth of cut: 0.3, 0.5, 0.7, 0.9, 1.1 mm for both the materials. No cutting fluid was used during the cutting tests. The selection of the cutting conditions i.e. cutting speed, feed and depth of cut was based on Sandvik coromant recommendations, although the cutting speeds were somehow limited by the sizes of the workpieces. Cutting conditions for the Taguchi experiments are as listed in the experimental results. Cutting conditions for the milling, grinding and EDM experiments are also as listed under the experiments.

3 Experimental Procedures.

Turning experiments were carried out on a Harrison M500 Engine Lathe using the standard throwaway -5^0 SCEA (CNG) and -1^0 SCEA (TNG) inserts. Surface roughness and cutting force measurements were initially carried out by traditional method mainly to observe the continuing trends of the process variables that were measurable. For each cutting test, the surface roughness produced was measured using MITUTOYO SURFTEST 301. The mean values of R_a were estimated from the three randomly taken measurements of the roughness across the feed marks. Following the surface roughness tests, cutting force experiments were carried out. A KISTLER dynamometer was used for in-process force measurements. Three components of the cutting force were recorded using the data acquisition system. Secondly, combined surface roughness and cutting force tests were carried out simultaneously using the Taguchi method. For all the trial tests, the resulting surface roughness was measured and cutting force recorded.

The milling experiments: Slabs of dimensions 140 mm x 35mm x 31 mm of XW-42 and 140 mm x 19 mm x 16 mm of ASP-23 were face milled with a fly cutter of diameter 20 mm on a vertical milling machine manufactured by LAGUN. The machining conditions are as follow: Rotational speed = 1000 rpm, Feed = 0.10 mm/tooth, Depth of cut = 0.5 mm. Cutting tool = TPKN 1603 PDSR-1CTIN 25 carbide type inserts manufactured by CANELA. After each experiment, the surface roughness on each workpiece was measured.

The grinding experiments: Each of the experimental workpieces as specified under the milling experiments was ground on a surface-grinding machine and the surface roughness measured. The machining conditions included the following:
Machine type: 63 DX OKAMOTO
Grinding wheel: Noritake grinding wheel
WA 60 J V 75 2000
Surface speed, V: 2000 m/min
Wheel dimension: 340 mm x 40 mm
Depth of cut: Rough downward feed = 10 μm
Intermediate feed = 0.5 μm
Finishing fine down feed = 0.1 μm

The EDM experiments: The EDM system consisted of a SW 25-electrode wire of 0.25 mm in diameter and a slab of an experimental workpiece connected, one at a time, to an ac power supply placed in distilled water. Each workpiece was clamped within the tank containing the fluid. Transient sparks were discharged through the fluid due to the potential difference between the tool and workpiece, removing a small amount of the metal from the workpiece surface. The duration of each experiment was 20 minutes. The surface roughness of each workpiece was measured.
Machining conditions:
Machine type: ROBOFIL 100 manufactured by Charmilles Technologies; Finishing 2; CH 24 E 6

Parameters:	M	C	V	P	A	F	WB
	7	0	-3	7	1	200	1200 gr

4 Results

4.1 High Carbon High Chromium Steel (XW - 42) turned with CNGN and TNGN inserts

From Figure 1, it could be seen that roughness R_a increases with speed up to 123 m/min for both inserts, but decreases with increasing speed from 123 to 192 m/min. Beyond this point, the CNG-insert shows a relatively sharp increase at 250 m/min.

The increase in R_a might have been caused by damage to the workpiece surface by the chip curling back into the work [8]. Chatter might be another cause [9]. The machined surface roughness for the TNG insert at 250 m/min is not marked. For sharp tools the equation for surface roughness is given by [10]:

$$h_{\max} = \frac{s}{Cot\,\kappa_1 + Cot\,\kappa_2} \qquad (1)$$

where K_1 = (90^0 – SCEA), K_2 = ECEA, and s = feed (mm/rev)

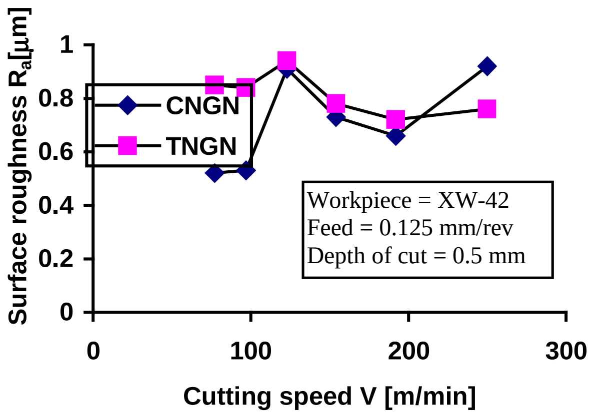

Figure 1. Cutting speed and surface roughness on High Carbon High Chromium Steel (XW-42). R_a is better with SCEA of -5°.

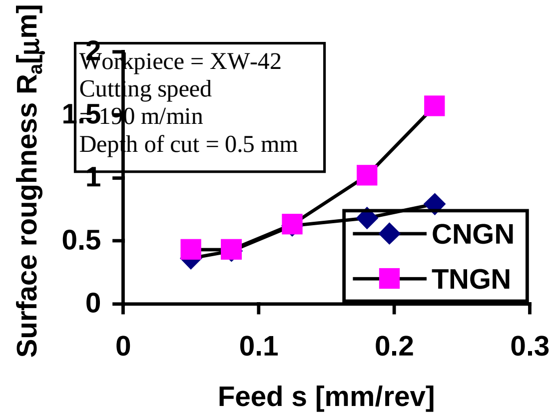

Figure 2. Feed and surface roughness on High Carbon High Chromium Steel (XW-42). R_a is better with SCEA of -5°.

Calculation of h_{max} indicates lower surface roughness with the -5^0 SCEA (CNG) insert. The relatively better surface roughness for the -5^0 SCEA (CNG) can be attributed to its lower SCEA and ECEA of -5^0 and 5^0 respectively, when compared to the -1^0 SCEA (TNG) insert having SCEA and ECEA of -1^0 and 6^0 respectively.

In Figure 2, R_a increases with feed for both inserts. However, the TNG insert shows higher roughness values beyond 0.125 mm/rev feed. In Figure 3, the inserts indicate relatively higher R_a values at the lower depth of cuts. At the low depth of cuts the metal being cut becomes too thin to be cut off, as observed by Jin-Hua [11]. In such a situation, the squeezing action on the workpiece by the round portion of the cutting edge could be intensified, thus increasing the friction and deformation and subsequent increase in the machined surface roughness. The increase in the R_a value at the lower depth of cuts might have been caused by squeezing action of the inserts on the workpiece. From 0.5 mm and 0.7 mm, R_a increases with depth of cut for the CNG-and TNG-inserts respectively as normally expected.

Using the Taguchi Method to obtain surface roughness on High Carbon High Chromium Steel (XW-42) workpiece, four factors considered in this work, are Tool Geometry, Cutting speed, Feed and Depth of cut. The cutting conditions are as follows:

Tool Geometry (A)	= TNG, CNG
Cutting speed (B)	= 116 m/min, 145 m/min
Feed (C)	= 0.05 mm/rev, 0.08 mm/rev
Depth of cut (D)	= 0.5 mm, 0.7 mm.

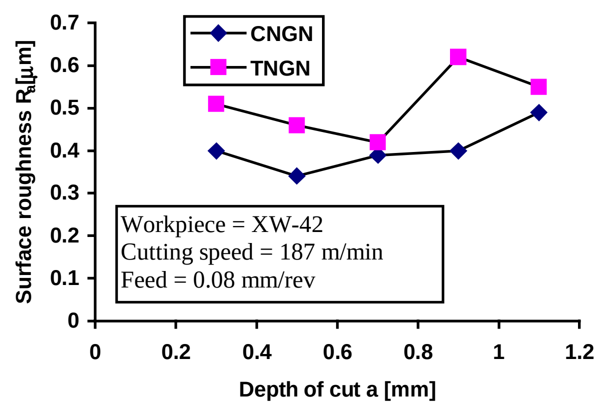

Figure 3. Depth of cut and surface roughness on High Carbon High Chromium Steel (XW-42). R_a is better with SCEA of -5°.

The surface roughness results obtained by the Taguchi method when turning XW-42 is depicted in Table 1. Although the CNG insert showed relatively better surface roughness by the traditional method, the TNG insert proved significant by the Taguchi method. The insignificant contribution of the cutting speed at the optimum condition during the process might have favoured the significant contribution of the TNG insert.

Figure 4 depicts the cutting force on XW-42 by the Traditional method. From the figure, it could be observed that the cutting force steadily increases with feed for both inserts. Usually the rake angle and side cutting edge angle (SCEA) play significant role in the mechanics of metal cutting operations. The rake angle determines the shear angle to a large extent. The shear angle influences the chip thickness, cutting force and power requirements, and temperature. With

Table 1. Estimation of Optimum Condition of Process : For Smaller the Better Characteristics.

Factor Description	Level Description	Level	Contribution
1 Tool Geometry A	TNG-insert	1	-0.056
4 Feed C	0.05 mm/rev	1	-0.057
Contribution from all factors (total)			-0.113
Current grand average of performance			0.383
Estimated result at optimum condition			0.270

Optimum Class Interval, C.I. = Sqr((F(n1, n2) * Ve)/Ne) where F(n1,n2) = computed value of F = 3; n1 = 1 (mean DOF, always 1), n2 = error DOC = 13; Ve = Error variance = 0.0054524, Ne = Effective number of Replications = 3.2, Confidence Level = 90%, Confidence Interval = $\pm$ 0.06783. Expected Result at Optimum Condition = 0.27 $\pm$ 0.06783 μm. Confirmatory test result = 0.28 μm. However, the confirmatory test result proved to lie within the interval of the expected result at the optimum condition at the specified confidence level.

decreasing rake angle, the shear angle decreases especially when cutting with a tool of negative rake angle [12].

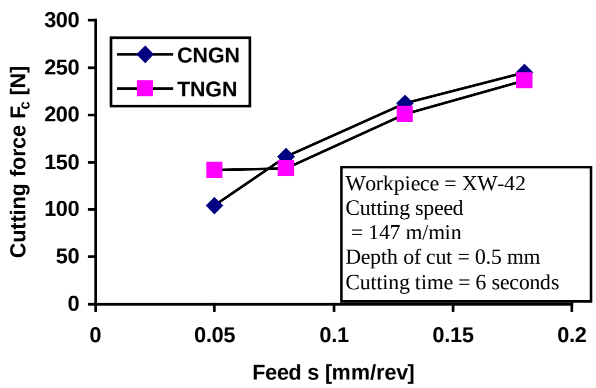

Figure 4. Feed variation with cutting force on High Carbon High Chromium Steel (XW-42). Cutting force is lower with SCEA of -1°.

This decrease in the shear results in a large shear plane and hence high cutting force and energy to shear the chip. The work of Venkatesh et al [7] has revealed that cutting forces, especially the radial force decreases with SCEA. The relatively low radial force Fp (Table 2) of the CNG insert at the lowest feed (0.05 mm/rev) could have contributed to the rigidity of the tool-work system that in turn resulted in lower cutting forces and even better surface roughness.

Beyond this feed, the radial force, effect does not seem to be very significant for both the inserts. The rake angle might have contributed to the differences in the cutting forces but to a minimal extent. This is because the difference in the rake angles i.e. -5^0 for the CNG and -6^0 for the TNG, of the two inserts is assumed too small. However, the effect of the rake angle cannot be ignored for the relatively lower cutting forces of the TNG insert at higher feeds. The SCEA has very little effect on the forces produced during the cutting process. In Figure 5, the cutting speed virtually has no effect on the cutting force for the CNG-insert but shows a slightly fluctuating decrease in the cutting force with speed is observed for the TNG-insert.

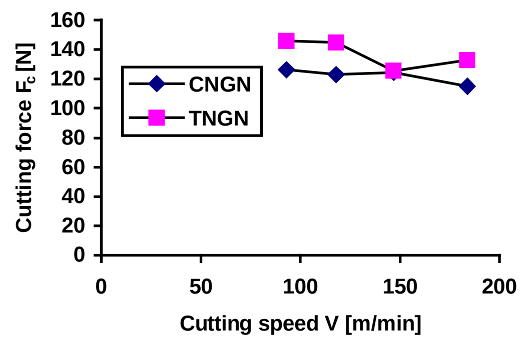

Figure 5. Cutting speed variation with cutting force on High Carbon High Chromium Steel (XW-42). Cutting force is lower with SCEA of -5°.

Table 3 depicts the results of the cutting force on XW-42 by Taguchi method.

Table 2. Force components of oblique cutting when XW-42 was turned.

Feed mm/rev	Turning XW-42 with TNG-insert			Turning XW-42 with CNG insert		
	Ff [N]	Fp [N]	Fc [N]	Ff [N]	Fp [N]	Fc [N]
0.05	75.95	104.52	141.95	41.24	88.34	103.88
0.08	53.35	116.07	143.37	84.30	105.17	155.69
0.125	78.82	179.77	200.67	66.48	144.73	211.94
0.18	66.98	173.89	236.16	73.45	174.61	244.87

Ff = Feed force, Fp = Radial force, Fc = Cutting force

Table 3. Estimation of Optimum Condition of Process : For Smaller the Better Characteristics.

Factor Description	Level Description	Level	Contribution
4 Feed C	0.05	1	-19.871
7 Depth of Cut D	0.5	1	-25.541
Contribution from all factors (total)			-45.411
Current grand average of performance			161.169
Estimated result at optimum condition			115.759

Optimum Class Interval: C.I. = Sqr((F(n1, n2) * Ve)/Ne), where F(n1,n2) = computed value of F = 3; n1 = 1 (mean DOF, always 1), n2 = error DOC = 13; Ve = Error variance = 234.48485400, Ne = Effective number of Replications = 3.2, Confidence Level = 90% ,Confidence Interval = $\pm$ 14.06579. Expected Result at Optimum Condition = 115.759 $\pm$ 14.06579N/mm^2.
Confirmatory test result = 125.66 N. Feed (0.05 mm) and depth of cut (0.5 mm) are significant. The confirmatory test result proved to lie within the interval of the expected result at the optimum condition at the specified confidence level.

4.2 Powdered High Speed Steel (ASP-23) turned with CNGN and TNGN inerts

In Figure 6, the machined surface roughness shows a decreasing trend with increasing speed up to 80 m/min for the CNG-insert. It almost remains constant beyond that speed. The variation of R_a with speed is not marked for the TNG-insert. This means that the cutting speed has very little influence on R_a for the TNG-insert on material ASP-23. The SCEA of the CNGN can be a significant factor during the cutting process for its relatively lower surface roughness beyond 80 m/min.

It can be observed from Figure 7 that the R_a increases as feed increases as generally expected. Nevertheless, the TNG-insert shows an increased R_a at feed below 0.05 mm/rev. At too small a feed, the feeding mechanism of the machine tool produces a stick-slip motion [11]. Such a motion could result in a relatively higher roughness value particularly at the 0.04 mm/rev. The machined surface roughness steadily increases as the depth of cut increases for both inserts in Figure 8, as generally expected.

From Table 4, it could be seen that the feed (0.05 mm/rev.) and CNG-insert are significant and have dormant influence on the finish of the machined material. Interaction occurred between the CNG insert and cutting speed during the cutting process. Confirmatory test result falls outside the range of the expected result at optimum condition at the specified confidence level. The cause of this discrepancy can be attributed to the size, 25.40 mm diameter of the material [13].

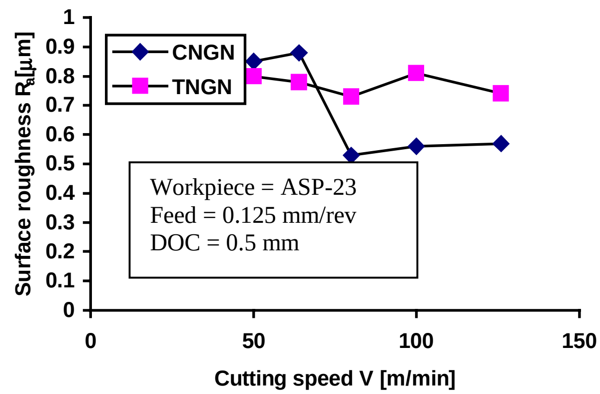

Figure 6. Cutting speed variation with surface roughness when Powdered High Speed Steel (ASP-23) was turned. R_a is better with SCEA of -5^o at higher speeds.

From Figure 9, it is observed that the cutting force steadily increases with feed for both inserts. The effect of the side cutting edge angle (SCEA) of the

CNG insert seems to be significant in this cutting process. This is evident in the relatively lower radial forces generated by the CNGN insert during the cutting process (Table 5).

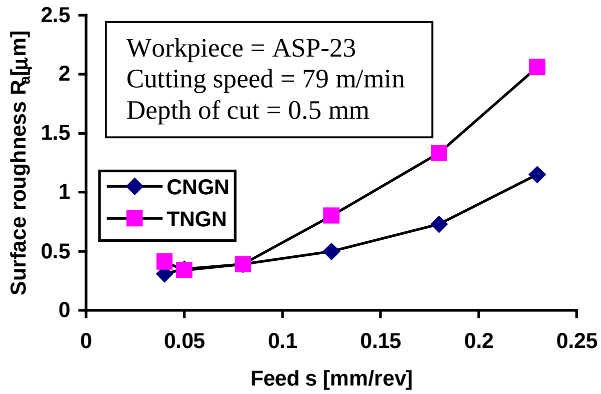

Figure 7. Feed variation with surface roughness when Powdered High Speed Steel (ASP-23) was turned. R_a is better with SCEA of -5^o especially at higher feeds.

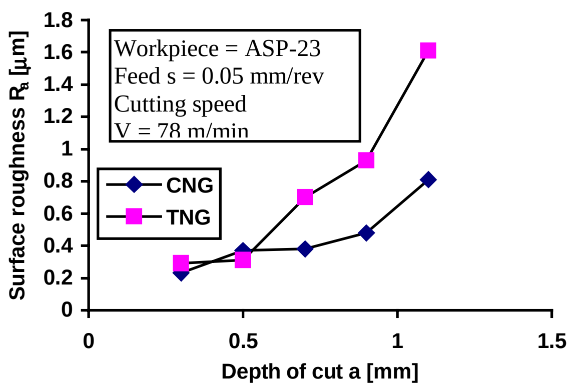

Figure 8. Depth of cut variation with surface roughness when (ASP-23) was turned. R_a is much better with SCEA of -5^o at higher depths of cut.

In Figure 10, the cutting force decreases with the speed for both inserts. The decreasing trend in the surface roughness as the cutting speed increases can be attributed to a cutting temperature increase and reduction in the friction coefficient [11].

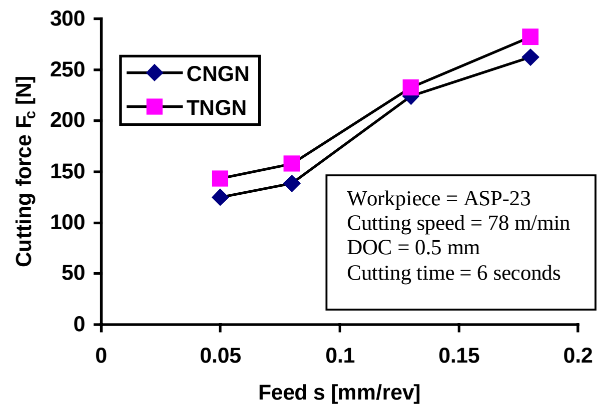

Figure 9. Feed variation with cutting force when ASP-23 was turned. Cutting force is lower with SCEA of -5^o .

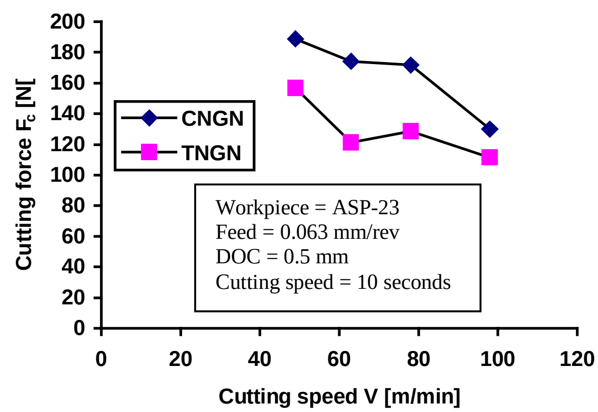

Figure 10. Cutting speed versus cutting force when ASP-23 was turned. Cutting force is much lower with TNGN of SCEA of -1^o.

The cutting force generated during the turning of ASP-23 material by Taguchi Method is displaced in Table 6, it could be observed that the feed of 0.05 mm/rev and depth of cut of 0.5 mm are significant and influenced the overall result. The confirmatory test result proved to lie within the interval of the expected result at optimum condition at the specified confidence level. However, the TNG insert seems to have played a significant role during the cutting process.

Table.4. Estimation of Optimum Condition of Process : For Smaller the Better Characteristics.

Factor Description	Level Description	Level	Contribution
1 Tool Geometry A	CNG	2	-0.093
2 Interaction (AxB)	N/A	2	-0.215
3 Feed C	0.05 mm/rev	1	-0.140
Contribution from all factors (total)			-0.448
Current grand average of performance			0.819
Estimated result at optimum condition			0.372

Optimum Class Interval: C.I. = Sqr((F(n1, n2) * Ve)/Ne), where F(n1,n2) = computed value of F = 4; n1 = 1 (mean DOF, always 1),n2 = error DOC = 4; Ve = Error variance = 0.0137375 ,Ne = Effective number of Replications = 1.6, Confidence Level = 90%, Confidence Interval = $\pm$ 0.17335. Expected Result at Optimum Condition = 0.372 $\pm$ 0.17335 m. Confirmatory test result = 0.78 m.

Table 5. Force components of oblique cutting when ASP-23 was turned.

Feed mm/rev	ASP-23 with TNG-insert			ASP-23 with CNG insert		
	Ff [N]	Fp [N]	Fc [N]	Ff [N]	Fp [N]	Fc [N]
0.05	56.82	118.64	143.28	66.71	96.56	124.90
0.08	80.79	146.58	157.92	67.61	109.89	138.48
0.125	71.12	176.84	232.32	92.59	167.10	224.01
0.18	72.12	218.64	282.08	68.89	209.12	262.24

Table 6. Estimation of Optimum Condition of Process : For Smaller the Better Characteristics.

Factor Description	Level Description	Level	Contribution
Tool Geometry A	TNG	1	-10.427
4 Feed C	0.05	1	-18.942
7 Depth of Cut D	0.5	1	-18.322
Contribution from all factors (total)			-47.701
Current grand average of performance			176.001
Estimated result at optimum condition			128.301

Optimum Class Interval: C.I. = Sqr((F(n1, n2) * Ve)/Ne), where F(n1, n2) = computed value of F = 3; n1 = 1 (mean DOF, always 1); n2 = error DOC = 12; Ve = Error variance = 268.74979063, NE = Effective number of Replications = 3.2, Confidence Level = 90%, Confidence Interval = $\pm$ 15.05847. Expected Result at Optimum Condition = 128.301 $\pm$ 15.05847N/mm^2
Confirmatory test result = 131.29 N

5 Discussion of Results

The Taguchi experiments, which followed the traditional experimental approach, were based on the trend of the results that were obtained from the latter experimental approach. The summary of the results is as shown in Table 7. The results of ceramic turning when compared with other machining processes are summarized in Table 8.

Table 7. The expected and confirmatory surface roughness and cutting force results.

Work Materials	Surface roughness [μm]		Cutting forces [N]	
	Expected results at optimum condition	Confirmatory test results	Expected results at optimum condition	Confirmatory test results
XW-42	0.27 ± 0.07	0.28	115.76 ± 14.07	125.66
ASP-23	0.37 ± 0.17	0.78	128.30 ± 15.06	131.29

Table 8. Ceramic turning compared with other machining processes.

Workpiece Materials	Surface roughness, R_a μm			
	Ceramic Turning	Carbide milling	Surface grinding	Wire EDM
XW-42	0.28	0.38	0.19	1.68
ASP-23	0.78	0.58	0.19	2.62

From Table 8, it can be observed that ceramic turning proved better than carbide milling for the XW-42 material. Despite the higher hardness of the ASP-23 (260 HB), the result of carbide milling proved better than ceramic turning. This discrepancy can be attributed to the smaller work material size of the ASP-23 when compared with the larger material size of the XW-42 for the turning operations. The grinding process showed better surface roughness results as expected when compared with ceramic turning. However, ceramic turning showed much better roughness values than the EDM process for both the materials, indicating its potential for milling moulds and die.

It is evident that differences do exist among the experimental results obtained. This can be expected because factors such as the composition and hardness differ among the experimental workpieces [3, 4, 8, 14]. The influence of the workpiece size [13] in particular is evident in the differences between the expected surface roughness result at optimum conditions and those of the confirmatory tests for the Powdered high speed steel (ASP-23) and XW-42 – Table 7. The nominal diameter of the ASP-23 was 25.4 mm compared with the High carbon high chromium steel (XW-42) workpiece material of diameter 50.8 mm. On the other hand, the workpiece size seems to have virtually little or no effect on the cutting force generation as observed by comparing the expected results at optimum condition with the confirmatory one of the ASP-23 material, Table 7. The SCEAs of the tools are also taught to have contributed to the variation of the surface roughness and cutting force results. However, the expected surface roughness results for both the work materials at optimum conditions are comparable with the range of standard surface roughness values for grinding operations [3, 8, 15,]. The experimental cutting force results are low compared with those values obtained when mild steel was turned with carbide inserts [16].

6 Conclusions

On the basis of the research findings, the following can be concluded.

1) Machining with the alumina TiC-based ceramic cutting tool
compares favourably with Electric Discharge Machining (EDM), milling with carbides and medium grinding processes, normally used in the fabrication of dies and moulds.
Furthermore results indicate that:
a) Ceramic turning proved better than electric-discharge machining (EDM).
b) Surface grinding of tool steels proved better than ceramic turning.
c) Taking work material size into consideration, ceramic turning is better than milling with carbide inserts and therefore milling with ceramics should be better than with carbides.
2) The excellent surface roughness obtained at higher feeds may have resulted from surface deformation due to burnishing action or occurrence of secondary shear, which were studied in this work.
3) A higher negative SCEA of -5^0 generally works better for the tool steels investigated than the -1^0. This can be attributed to the relatively lower radial force giving the tool stability, which is evident from the best roughness and cutting force values. In some cases, however, the -1^0 is better.

7 References

1. Whitney, E.D., New Advances in Ceramic Tooling, edited by Kane, G.E., Modern trends in cuttings tools, Dearborn, pp 91-98, 1982.
2. Schmidt, A.O., Cutting Tool Material Selection, Edited by Swinehart, H.J, American Society of Tool and Manufacturing Engineers, Dearborn, 1968.
3. Juneja, B.L., & S.Sekhon, G.S., Fundamentals of Metal Cutting and Machine Tools, Wiley Eastern Ltd., New Delhi, 1987.
4. Kalpakjian, S., Manufacturing Engineering and Technology, Addison-Wesley Publishing Company, U.S.A., 1995.
5. Shaw, M.C., Metal cutting principles, Clarendon Press, Oxford, 1984.
6. Jawahir, I.S., Qureshi, N., and Arsecularatne, On the interrelationships of some machinability parameters in finish turning with Cerment chip forming tool inserts, International Journal of Machine Tools and Manufacture, Pergamon Press Ltd., UK, Vol 32, No.5, pp 709-723, 1992.
7. Venkatesh, V.C., Kattan, L.A., Hoy, D., Ye C.T. and Vankirk, J.S., An analysis of cutting with negative side cutting edge angles. Journal of materials processing technology 58, pp351-361, 1996.
8. Groover M.P., Fundamental of Modern Manufacturing, Prentice-Hall International, Inc., U.S.A., 1996.
9. Jack, D.H., Ceramic Tool Materials, Edited by Schwartz Mel M., Engineering Applications of Ceramic Materials, American Society for Metals, U.S.A., pp 192-199, 1985.
10. Bhattacharyya, A., and Ham, I., Design of cutting tools, ASTME Publication, Dearborn, Mi., U.S.A, 1969.

11. Jin-Hua, Z., Theory and Technique of Precision Cutting, Pergamon Press, U.K., 1990.
12. Schey, A.J., Introduction to Manufacturing Processes, 2nd Edition, McGraw-Hill Book Company, Singapore, 1987.
13. Lea, F.C., and Simons, E.N., The Machining of Steels, ODHAMS Press Limited, London, 1960.
14. Hoffran, E.G., Jig and Fixture Design, 3rd Edition, Delman Publishing Inc., N.Y., 1991.
15. Whitehouse, D.J., Handbook of Surface Metrology, IOP Publishing Ltd., UK, pp 648-658, 1994.
16. Schweizer, U., Metal cutting-Force *measurements and calculation in turning operation, Kistler Training Center, 20.9014e 294 S, pp 1-13, 1994.*